Available online at www.sciencedirect.com
SCIENCE DIRECT®
Journal of Power Sources 138 (2004) 283–287
JOURNAL OF POWER SOURCES
www.elsevier.com/locate/jpowsour

Short communication

Self-discharge analysis of $LiCoO_2$ for lithium batteries

Sun Hee Choi[a], Joosun Kim[a], Young Soo Yoon[b,*]

[a] *Nano-Materials Research Center, Korea Institute of Science and Technology, P.O. Box 131, Cheongryang, Seoul 130-650, South Korea*
[b] *Department of Advanced Fusion Technology, Center for Emerging Wireless Power Transmission Technology, Konkuk University, Seoul 143-701, South Korea*

Received 4 June 2004; accepted 28 June 2004
Available online 27 August 2004

Abstract

In the charged condition, batteries are in a state of high energy relative to that of the system in the discharged state. Hence, there is a 'driving force', corresponding to the free energy of discharge, which tends to spontaneously diminish the charge if some mechanisms for self-discharge exist. We determined the self-discharge of $Li/LiCoO_2$ cells from the decline of their open-circuit voltage and the rate of loss of the discharge capacity. In addition, we studied ac impedance of $Li/LiCoO_2$ cells. Prevention of self-discharge is especially important for munitions that have remained in a state of disuse. In the case of nanocrystalline $LiCoO_2$, cycle performance is superior to coarse-grained $LiCoO_2$. However, self-discharge performance is inferior to coarse-grained $LiCoO_2$. A better cycle performance of up to 200 cycles might be due to a well-formed SEI layer and smaller particle size in nanocrystalline $LiCoO_2$.

Keywords: Lithium cobalt oxide; Li-ion battery; Self-discharge

1. Introduction

$LiCoO_2$ heat-treated above 700 °C (HT-$LiCoO_2$) has a high cycle life compared to other cathode materials, such as $LiNiO_2$ and $LiMn_2O_4$. The structure of $LiCoO_2$ is rhombohedral (R3m space group) with lattice parameters $a = 2.816$ Å and $c = 14.051$ Å in a hexagonal setting. The lattice is formed by oxygen atoms in ABC stacking with alternating layers of Li and Co ions in octahedral interstitial sites between the oxygen planes [1–4]. Combination of salt encapsulation with an earlier proposed powder engineering technique [5,6] ensures fine particle size control of $LiCoO_2$ powders obtained using wet chemical methods [7].

Charged batteries are in a state of high free energy relative to that of the discharged state, so there is a 'driving-force' for their 'self-discharge' as illustrated in Fig. 1, if appropriate mechanisms are available for passage of Faradaic currents. When batteries are charged and then left on open-circuit, a certain degree of 'self-discharge' can set in depending on the chemistry and electrochemistry of the system, the purity of reagents and electrolyte, and the temperature. In ideal batteries, electrons move through the external circuit, while some electrons move through the electrolyte in real batteries. This phenomenon is called 'self-discharge'. The rate of self-discharge, which usually diminishes with time, determines what is called the 'shelf life' of batteries which is especially important in the case of primary cells which are sold in the charged condition and stored as inventory. Some battery systems have an excellent shelf life, e.g. $Li/SOCl_2$ primaries, while others such as NiOOH/Cd or NiOOH/Zn have a substantially poorer shelf life in the charged state due to self-discharge processes [8].

In order to maintain 'full charge', a 'float current' of small magnitude can be applied to the charge storage system to balance the self-discharge rate. However, this brings about technological and hardware complexities, so minimization of the intrinsic self-discharge rates is desired. In this work,

* Corresponding author. Tel.: +82 2 2049 6042; fax: +82 2 452 5558.
E-mail address: ysyoon@konkuk.ac.kr (Y.S. Yoon).

0378-7753/$ – see front matter © 2004 Elsevier B.V. All rights reserved.
doi:10.1016/j.jpowsour.2004.06.047

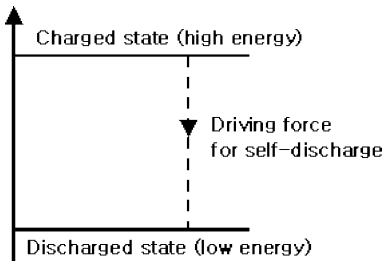

Fig. 1. Illustrates the driving force for self-discharge of a battery.

we focused our attention on the self-discharge of Li/$LiCoO_2$ cells with different $LiCoO_2$ particle sizes.

2. Details of experiment

An aqueous solution of Li and Co acetates (Li/Co = 1.1) was frozen with a spray of liquid nitrogen followed by freeze drying for two days at $P = 5 \times 10^{-2}$ mbar (Alpha 2–4, Christ). A part of the freeze-dried product was mixed with K_2SO_4 (1:10) and subjected to planetary milling (Pulverisette-5, Fritsch) in ZrO_2 media at 600 rpm for 24 h (ball to powder mass ratio of 10:1). Thermal decomposition of a precursor and of a precursor mixture with K_2SO_4 was performed in air first at 400 °C for 10 h, then at 800 °C for 12 h. The thermally processed mixture was washed with distilled water several times to eliminate SO_4^{2-} ions; $LiCoO_2$ residue was separated by centrifuging.

Obtained $LiCoO_2$ powders have been studied by XRD (Geigerflex, Rigaku, 2° min^{-1}, Cu Kα), scanning electron microscopy (SEM, Philips ESEM), and TEM (Philips CM-30, U = 200 kV). Commercial $LiCoO_2$ powder, supplied by Seimi Co., was used for comparison.

Electrochemical characterizations were performed using a CR2032 coin-type cell with the following parameters: cut-off voltage 3.2–4.2 V and I = 0.5 mA/cm^2 at room temperature. The cathode was fabricated with 20 mg of accurately weighed active material and 12 mg of conductive binder (8 mg of teflonized acetylene black (TAB) and 4 mg graphite). The cathode was pressed on 200 mm^2 stainless steel mesh, which was used as the current collector, under a pressure of 300 kg/cm^2 and subsequently dried at 180 °C for 24 h in a vacuum oven. The test cell was made of a cathode and a lithium metal as an anode separated by a porous polypropylene film (Celgard 3401). A mixture of 1 M $LiPF_6$-ethylene carbonate (EC)/dimethyl carbonate (DMC) (1:1 by vol., Merck) was used as the electrolyte.

Impedance of the battery cells was measured with a Solatron impedance system consisting of an SI 1287 Electrochemical Interface, a SI 1260 Impedance/Gain-Phase Analyzer, and a Pentium PC running a Zplot and ZView software by Scribner and Associates, Inc. The impedance measurement covered a frequency range from 5 to 100 kHz with an ac oscillation of 30 mV and with the dc bias voltage matching the OCV of the battery cell whose impedance was to be measured.

3. Results and discussion

SEM analysis of the $LiCoO_2$ powders, obtained by matrix isolation of precursor particles by K_2SO_4, confirmed the efficiency of this method in terms of grain coarsening prevention. Commercial Seimi Co. powder (powder A) formed micron-sized crystallites (Fig. 2A), while K_2SO_4-processed powder (powder B) was characterized by a grain size distribution in a range of 30–70 nm (Fig. 2B).

XRD analysis of coarse-grained (powder A) and nanocrystalline powders (powder B) revealed the formation of single phase hexagonal HT-$LiCoO_2$ in both cases (Fig. 3). Processing of $LiCoO_2$ powders at 800 °C in contact with K_2SO_4 was not accompanied by formation of secondary phases or by significant displacement of the main reflections displayed in the formation of solid solutions. Sharp and well-resolved

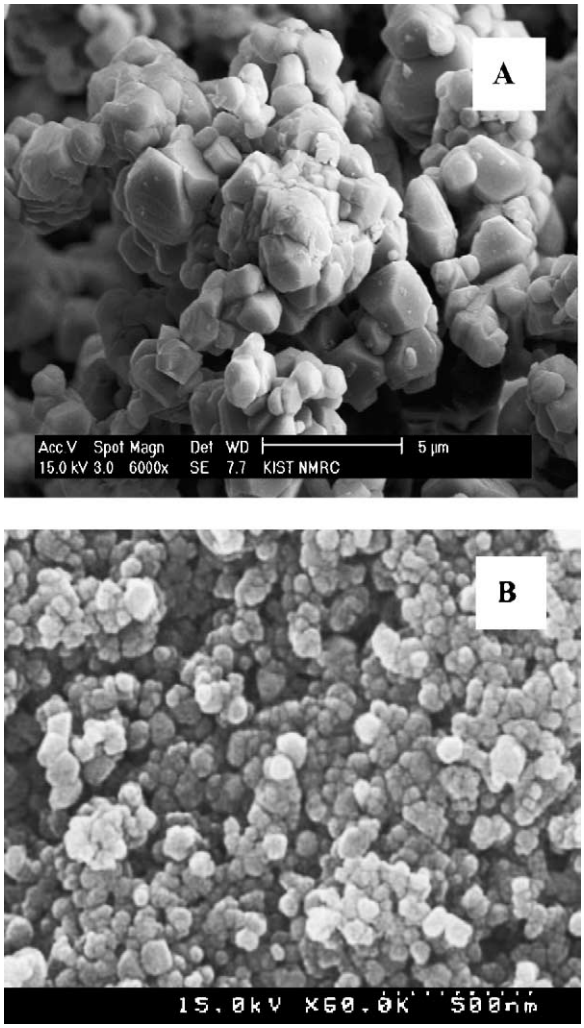

Fig. 2. SEM micrographs of (A) $LiCoO_2$ powders, Seimi Co. and (B) planetary processing with K_2SO_4.

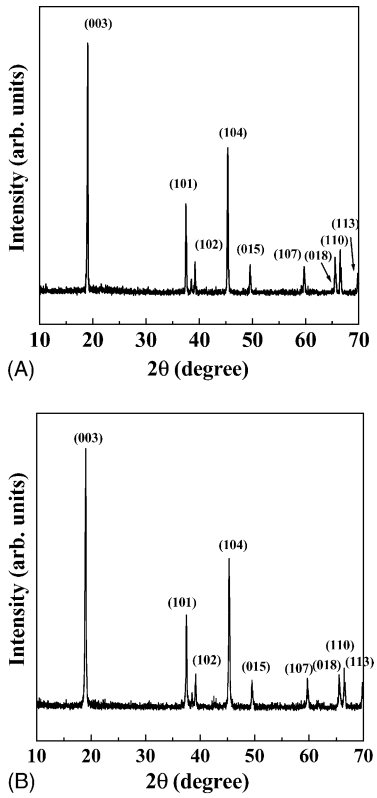

Fig. 3. XRD patterns of (A) coarse-grained Seimi Co. and (B) nanocrystalline $LiCoO_2$ powders.

reflections of both patterns were observed at perfect crystallographic ordering. The uncharacteristic (0 0 3)/(1 0 4) peak ratio for the nanocrystalline powder can be related to anomalies of element distribution within the Co sublattice [9].

Fig. 4 shows the cycle performance of coarse-grained (powder A) and nanocrystalline (powder B) $LiCoO_2$ cathode. The initial discharge capacity of powder B is smaller than that of powder A. The smaller discharge capacity is due to the partial cubic spinel phase in powder B [10]. Since the cubic spinel phase is less electrochemically active, its formation could be a source of the capacity loss. However, the cycle life of powder B up to 200 cycles is better than that of powder A. The superior cycle performance of powder B is due to the smaller particle size. Smaller particle size ensures shorter mean length of Li diffusion pathways from its position in the $LiCoO_2$ lattice to the cathode–electrolyte interface. Also, diffusion through the grain boundary of powder B is larger than that of powder A. Shorter diffusion distances promote faster and more uniform Li intercalation into $LiCoO_2$ crystallites during the discharge process compared to powder A, thus increasing the effective capacity values.

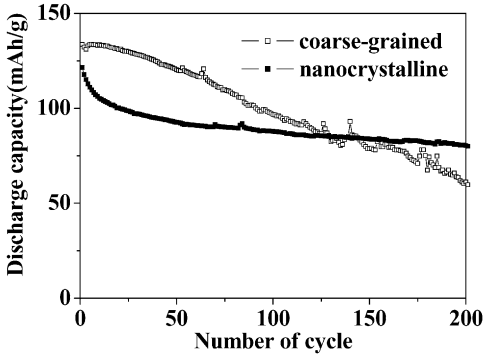

Fig. 4. Cycle performance for coarse-grained Seimi Co. and nanocrystalline $LiCoO_2$ cathodes.

To study the self-discharge of the Li/$LiCoO_2$ battery cells, we observed the decline of OCV of freshly prepared cells after charging them to 4.2 V at a rate of 0.5 mA/cm^2. OCV decline of two different Li/$LiCoO_2$ cells (coarse-grained $LiCoO_2$ and nanocrystalline $LiCoO_2$) are almost the same, 4.04 and 4.07 V, respectively for the period of one month. The rate of preservation of discharge capacity of coarse-grained $LiCoO_2$ is 83.1%, while that of nanocrystalline $LiCoO_2$ is 80.7%. To avoid the possibly negative effect of reducing grain size below 100 nm deal with a substantially enhanced surface area of nanopowders, accelerating catalyst decomposition of the electrolyte at the surface of cathode material. Li^+ ions generated from the decomposition of the electrolyte move into $LiCoO_2$ lattice. Smaller particle size ensures shorter mean length of Li diffusion pathways. Therefore, the degree of self-discharge of nanocrystalline $LiCoO_2$ is larger than that of coarse-grained $LiCoO_2$. The higher discharge capacity of coarse-grained $LiCoO_2$ in Fig. 4 also includes the effect of high rate of preserving the discharge capacity during 100 cycles.

The impedance spectrum is generally composed of three partially overlapping semicircles in the high, medium and low frequency regions, and a straight sloping line in low frequency regions. From high to low frequencies, these three semicircles can be respectively assigned to the spectra of the cell bulk impedance, SEI film impedance, and charge-transfer process [11,12]. Each spectrum in Fig. 5 can be fitted with an electric circuit consisting of a resistor and a parallel capacitor. R_s (R_1 + R_2) is ascribed to the sum of the ionic resistance of the electrolyte (R_1) and electronic resistance of the electrodes (R_2). R_f and C_f are the resistance and capacitance of the SEI film; R_{ct} and C_{dl} are the charge-transfer resistance and the double-layer capacitance; W is the Warburg impedance related to the diffusion of lithium ions in the electrodes [13].

Fig. 5(A) compares the impedance spectra of the cell with coarse-grained $LiCoO_2$ and nanocrystalline $LiCoO_2$ in its fully charged state. Another possible negative effect of reducing grain size below 100 nm deals with poorer electrical contacts between particles when it concerns phases with low electronic conductivity. In Fig. 5, electronic resistance of electrode (R_2) of nanocrystalline powder is slightly larger than that of coarse-grained powder. We found two semicircles at high and medium frequency regions in coarse-grained $LiCoO_2$, while finding only one semicircle in the high frequency region in nanocrystalline $LiCoO_2$. Although the resistance of the SEI film is 26 Ω in coarse-grained $LiCoO_2$, the resistance of the SEI film does not exist in nanocrystalline

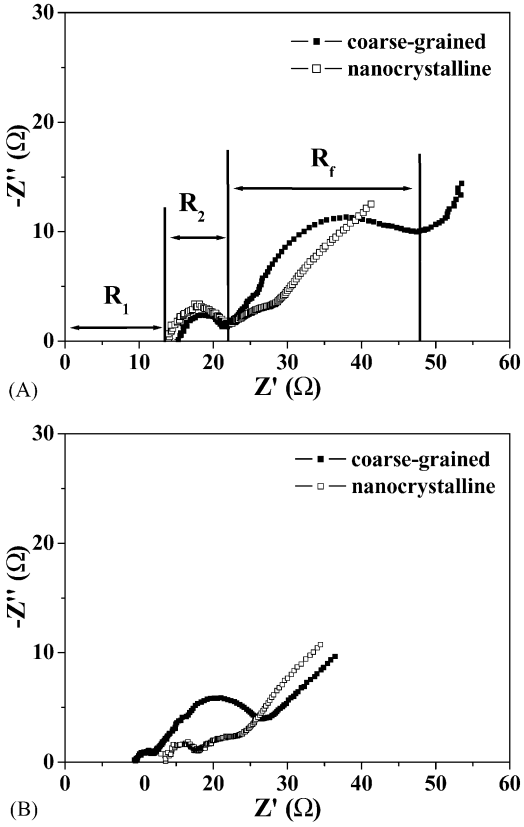

Fig. 5. Impedance curves of Li/$LiCoO_2$ cells for coarse-grained Seimi Co. and nanocrystalline $LiCoO_2$ cathodes (A) at a fully charged state and (B) at a self-discharged state.

$LiCoO_2$. This shows it is likely that products of parasitic reactions collect on the surface of cathode material at a faster rate in coarse-grained $LiCoO_2$. As a result, the total thickness of the surface film increases quickly. In both cases, the R_{ct} is very high and its corresponding impedance spectrum changes into a straight sloping line. As a result, R_{ct} is too large to be measured.

Two recent publications give indications of the presence of an SEI layer on the cathode [14,15]. Balasubramanian et al. [16] reported on soft X-ray absorption spectroscopy (XAS) studies on cathodes. Based on the XAS, the presence of LiF compounds in the cathode SEI was inferred in $LiPF_6$-based electrolytes. The most likely source for LiF comes from the decomposition of $LiPF_6$ according to the reaction

$$LiPF_6 \rightarrow PF_5 + LiF$$

The precipitated LiF is the most likely major contributor to the insulating layer [17]. Precipitation of LiF could affect ionic motion by pore plugging, or could contribute to resistive electrical paths to parts of the cathode structure. At the cathode organic decomposition products are unstable, particularly on charged cathodes. This permits the formation of a dense LiF coating [16]. The well-formed SEI layer, by adding various additives, could suppress the decomposition of electrolyte solvents, which prohibited the leakage of electrolyte and improved the cycling performance of lithium ion batteries [18,19]. Therefore, in case of coarse-grained $LiCoO_2$, higher discharge capacity and better cycle performance until 100 cycles might also be due to a well-formed SEI layer.

Fig. 5(B) compares the impedance spectra of the cell with coarse-grained $LiCoO_2$ and nanocrystalline $LiCoO_2$ in its self-discharged state. We also found two semicircles at high and medium frequency regions in coarse-grained $LiCoO_2$, but found only one semicircle at high frequency region in nanocrystalline $LiCoO_2$. The resistance of the ionic resistance of the electrolyte and electronic resistance of the electrodes decreased in coarse-grained $LiCoO_2$. The resistance of the electrodes decreased in nanocrystalline $LiCoO_2$. The resistance R_s decreased because some electrons move through the electrolyte during self-discharge. The resistance of the SEI film is 14 Ω in coarse-grained $LiCoO_2$, while the resistance of the SEI film does not exist in nanocrystalline $LiCoO_2$. In case of coarse-grained $LiCoO_2$, the resistance of the SEI film reduced from 26 to 14 Ω during self-discharge. In both cases, the R_{ct} is also very high and its corresponding impedance spectrum changes into a straight sloping line.

Fig. 6(A) compares the impedance spectra of the cell with coarse-grained $LiCoO_2$ and nanocrystalline $LiCoO_2$ in the fully discharged state. We found one semicircle at medium frequency regions in coarse-grained and nanocrystalline $LiCoO_2$. While the resistance of the SEI film is 28 Ω in coarse-grained $LiCoO_2$, the resistance of the SEI film is 9 Ω in nanocrystalline $LiCoO_2$. Compared to self-discharged

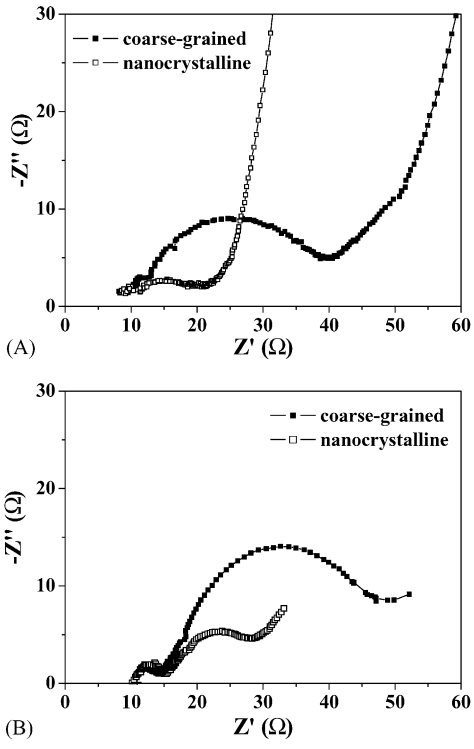

Fig. 6. Impedance curves of Li/$LiCoO_2$ cells for coarse-grained Seimi Co. and nanocrystalline $LiCoO_2$ cathodes (A) at a fully discharged state and (B) at a charged state after 46 cycles.

state, the resistance of the SEI film increased again. In both cases, the R_{ct} is very high and its corresponding impedance spectrum changes into a straight sloping line. As a result, R_{ct} is too large to be measured. There is driving force for self-charge in a fully discharged state as well as a driving force for self-discharge in fully charged state. Fig. 6(B) compares the impedance spectra of the cell with coarse-grained $LiCoO_2$ and nanocrystalline $LiCoO_2$ in fully charged state after 46 cycles. There is also SEI impedance in nanocrystalline $LiCoO_2$. Therefore, better cycle performance up to 200 cycles might be due to a well-formed SEI layer and smaller particle size in nanocrystalline $LiCoO_2$.

4. Conclusion

We determined the self-discharge of Li/$LiCoO_2$ cells from the decline of their open-circuit voltage and the preservation of discharge capacity. In addition, we studied ac impedance of Li/$LiCoO_2$ cells. In case of nanocrystalline $LiCoO_2$, cycle performance was superior to coarse-grained $LiCoO_2$. However, self-discharge performance was inferior to coarse-grained $LiCoO_2$. The resistance of the SEI film existed in coarse-grained $LiCoO_2$, while the resistance of the SEI film did not exist in nanocrystalline $LiCoO_2$. In case of coarse-grained $LiCoO_2$, the resistance of the SEI film decreased during self-discharge and increased again at its fully discharged state. There is a driving force for self-charge in its fully discharged state as well as a driving force for self-discharge in the fully charged state. There is also SEI impedance in nanocrystalline $LiCoO_2$ after 46 cycles. A better cycle performance until 200 cycles might be attributed to a well-formed SEI layer and smaller particle size in nanocrystalline $LiCoO_2$.

Acknowledgements

We would like to express our utmost appreciation for R&D support provided by the Korean government's National Research Laboratory Program (Development of monolithic high power hybrid battery).

References

[1] W.D. Johnston, R.R. Heikes, D. Sestrich, J. Phys. Chem. Solids 7 (1958) 1.
[2] K. Mizushima, P.C. Jones, P.J. Wiseman, J.B. Goodenough, Mater. Res. Bull. 15 (1980) 783.
[3] H.J. Orman, P.J. Wiseman, Acta Crystallogr. C40 (1984) 12.
[4] T.A. Hewston, B.L. Chamberland, J. Phys. Chem. Solids 48 (1987) 97.
[5] V.V. Ischenko, O.A. Shlyakhtin, N.N. Oleinikov, et al., Physica C 282–287 (1997) 855.
[6] Y.D. Tretyakov, N.N. Oleinikov, O.A. Shlyakhtin, Cryochem. Technol. Adv. Mater., Chapman & Hall, London, 1997.
[7] O.A. Shlyakhtin, Y.S. Yoon, Y.-J. Oh, J. Eur. Ceram. Soc. 23 (2003) 1893.
[8] B.E. Conway, W.G. Pell, T-C. Liu, J. Power Sources 65 (1997) 53.
[9] K. Kanamura, A. Goto, R.Y. Ho, et al., Electrochem. Solid State Lett. 3 (2000) 256.
[10] S.H. Choi, J.S. Kim, Y.S. Yoon, J. Korean Ceram. Soc. 41 (2004) 86–91.
[11] S.S. Zhang, M.S. Ding, K. Xu, J.L. Allen, T.R. Jow, Electrochem. Solid State Lett. 4 (2001) A206.
[12] S.S. Zhang, K. Xu, T.R. Jow, Electrochem. Solid State Lett. 5 (2002) A92.
[13] S.S. Zhang, K. Xu, J.L. Allen, T.R. Jow, J. Power Sources 110 (2002) 216.
[14] Y. Wang, X. Guo, S. Greenbaum, J. Liu, K. Amine, Electrochem. Solid State Lett. 4 (2001) 68.
[15] D. Ostrovskii, F. Ronci, B. Scrosati, P. Jacobsson, J. Power Sources 94 (2001) 183.
[16] M. Balasubramanian, H.S. Lee, X. Sun, X.Q. Yang, A.R. Moodenbaugh, J. McBreen, D.A. Fischer, Z. Fu, Electrochem. Solid State Lett. 5 (2002) A22.
[17] R. Kostecki, X. Zhang, P.N. Ross, Jr., F. Kong, S. Sloop, J.B. Kerr, K. Striebel, E. Cairns, F.R. McLarnon, Abstract 190, The Electrochemical Society Meeting Abstracts, vol. 2000–2002, Phoenix, AZ, October 22–27, 2000.
[18] C. Wang, H. Nakamura, H. Komatsu, M. Yoshio, H. Yoshitake, J. Power Sources 74 (1998) 142.
[19] G.H. Wrodnigg, C. Reisinger, J.O. Besenhard, M. Winter, ITE Battery Lett. 1 (1999) 110.